Soil Biology and Biochemistry 185 (2023) 109147

Contents lists available at ScienceDirect

Soil Biology and Biochemistry

journal homepage: www.elsevier.com/locate/soilbio

A new concept for modelling the moisture dependence of heterotrophic soil respiration

Zhongdong Huang [a], Yuan Liu [a,*], Pengfei Huang [a], Zhongyang Li [a,b], Xiaoxian Zhang [c]

[a] Institute of Farmland Irrigation, Chinese Academy of Agricultural Sciences, Xinxiang, 453002, Henan Province, China
[b] National Research and Observation Station of Shangqiu Agro-ecology System, Shangqiu, 476000, China
[c] Sustainable Soils and Crops, Rothamsted Research, Harpenden, Hertfordshire, AL5 2JQ, UK

ARTICLE INFO

Keywords:
Heterotrophic soil respiration
Pore-scale substrate heterogeneity
Macropores
Modelling
Oxygen dissolution and diffusion
Moisture and temperature response

ABSTRACT

The moisture dependence of heterotrophic soil respiration is a key factor affecting the uncertainty in predicting the response of soil organic carbon (SOC) to global warming. Considering that heterotrophic respiration from unsaturated soils is primarily driven by microbial reduction of oxygen (O_2), we propose a new concept to model the respiration by tracking dissolution of gaseous O_2 and its subsequent diffusion and microbial reduction at hydrated microsite in the pore space of soil. Total respiration from a soil sample is calculated by summing the O_2 reduced by all microbes in the soil. This allows us to separate physical processes and microbial activity occurring at microsites and incorporate pore-scale substrate heterogeneity, macropores and other factors explicitly into the model. We show that scaling up these microscopic physical processes over a soil sample makes soil moisture, temperature, and other factors inherently integrated in their influence on microbial respiration, and that a change in one of them affects the response of the respiration to the change in others. Comparison with experimental data shows the model can reproduce the diverse moisture-respiration relationships observed from various experiments and predict the change in soil respiration with temperature. It is noteworthy to point out that previous studies had attributed the variations in the moisture and temperature sensitivity of heterotrophic soil respiration to microbial adaptation; herein we demonstrate that changes in soil structure and physical processes can also give rise to such variations. Distinguishing between physical and microbial effects in data analysis and modelling is therefore crucial, as mistaking physical effects for microbial adaptation would lead to errors in predicting the response of SOC to environmental changes.

1. Introduction

Soil water and temperature are the two most critical abiotic factors influencing biogeochemical processes and the sensitivity of soil organic carbon (SOC) to environmental changes in terrestrial ecosystems. While temperature primarily affects microbial metabolism, the impact of soil water is multifaceted and diverse (Moyano et al., 2013). In addition to keeping microbes hydrated, soil water also functions as a medium for exoenzymes and soluble substrates to move away and towards microbes. For respiration of aerobic microbes, soil water controls bioavailability of oxygen (O_2), as O_2 becomes bioavailable only after it dissolves at water-air interface and diffuses to regions in close proximity of microbes (Lee et al., 2003). These physical processes are modulated by soil structure and temperature, as temperature rise reduces O_2 dissolution at water-air interface while a change in soil structure alters the water-air interface for O_2 to dissolve and the distance between water-air interface and microbes for dissolved O_2 to move (Zhang et al., 2022). Correctly representing these physical processes in SOC models is critical to reliably projecting the response of SOC to global warming but challenging because of their complexity (Falloon et al., 2011).

Most SOC models currently in use parameterize the soil water effect using a moisture function to scale back the heterotrophic respiration achieved at an optimal moisture content for microbial respiration (Bauer et al., 2008; Moyano et al., 2013). Since the mechanisms responsible for emergence of the optimal water content are diverse and difficult to quantify, most moisture functions are phenomenological and vary widely between SOC models (Bauer et al., 2008). Skopp et al. (1990) made the first effort to mechanistically describe the soil moisture effect

* Corresponding author.
E-mail addresses: huangzhongdong@caas.cn (Z. Huang), liuyuanfiri88@163.com (Y. Liu), huangpengfei@caas.cn (P. Huang), lizhongyang1980@163.com (Z. Li), xiaoxian.zhang@rothamsted.ac.uk (X. Zhang).

https://doi.org/10.1016/j.soilbio.2023.109147
Received 22 April 2023; Received in revised form 3 July 2023; Accepted 8 August 2023
Available online 12 August 2023

on respiration, and Yan et al. (2018) improved it. Although the models developed by them differ mathematically, their physical principles are comparable in that the variation in respiration with soil moisture is the compromise between gaseous O_2 diffusion and aqueous O_2 diffusion. They defined a critical moisture content when gaseous O_2 diffusion and aqueous O_2 diffusion are in balance. To derive the moisture function, it was assumed that when soil water content is lower than the critical value, the respiration is limited by aqueous O_2 diffusion, while when soil water content is higher than the critical value, gaseous O_2 diffusion is the limiting factor. This is an approximation, as the relative dominance of the gaseous and aqueous O_2 diffusions in their influence on the respiration should undergo a transition rather than an abrupt change over the critical moisture, as demonstrated by theoretical analysis and experimental data (Zheng et al., 2022).

Emission of CO_2 from soils is the result of microbial metabolism. Although denitrification and fermentation in wet soils and oxidation of methane also produce CO_2 (Tokida et al., 2011; Guilhen et al., 2020), in unsaturated soils, the main source of CO_2 is microbial reduction of O_2 (Skopp et al., 1990; Yan et al., 2018; Zhang et al., 2022). Physically, atmospheric O_2 moves into the soil first, and then dissolves and diffuses in water in the hydrated pore space before being microbially reduced at reactive sites. During these processes, O_2 needs to overcome various resistances. Since gaseous O_2 moves four-five orders of magnitude (depending on temperature and atmospheric pressure) faster than dissolved O_2, O_2 dissolution and its subsequent diffusion are the mechanisms underlying the transition between anaerobic and aerobic environment in soils (Keiluweit et al., 2017; Harris et al., 2021). Assuming microbes reside on the wetted pore walls, Zhang et al. (2022) proposed a model showing that temperature and soil water are nonlinearly coupled in their influence on soil respiration. While the assumption is rational, some microbes in soils are not static but motile (Ebrahimi and Or, 2016). In this paper, we propose to calculate the effect of soil water on heterotrophic soil respiration by modelling diffusion of dissolved O_2 and its microbial reduction in hydrated pore space as two random processes. The model for microbial respiration from a soil sample is derived from the mass balance that at equilibrium, the mass of O_2 dissolved at water-air interface in the soil sample is the same as the O_2 reduced by microbes in the soil. We compare the model with various experiments with both moisture and temperature gradients and discuss the importance of explicitly including these physical processes in data interpretation and modelling the response of SOC to environmental changes.

2. Model development

2.1. Theoretical analysis

Fig. 1A shows schematically the microscopic cross-section of a soil with water and air co-existing in its pore space. As water in soil is held by capillary pressure, water is in small pores and air in large pores. Gaseous O_2 diffuses four-five orders of magnitude faster than dissolved O_2, and the partial pressure of gaseous O_2 in the soil sample can thus be assumed to be spatially uniform. Gaseous O_2 dissolves at the water-air interface and then moves randomly in the hydrated pore space (Fig. 1B). If a gaseous O_2 molecule dissolves at water-air interface at time $t = 0$, in the absence of biogeochemical reactions, the probability that it is still in water without being evaporated after time elapses to t is represented by $g_1(t)$. In literature, $g_1(t)$ is known as memory function (Haggerty and Gorelick, 1995; Li et al., 2018). When microbes are present and the reduction of O_2 by microbes can be approximated by a first-order kinetic with the kinetic reaction rate represented by k_c, the probability that the O_2 molecule has not been respired by microbes at time t is $g_2(t) = \exp(-k_c t)$ (Li et al., 2018). Because O_2 movement and its microbial reduction are independent, under the combined impact of random movement and microbial reduction, a O_2 molecule that dissolves at water-air interface and is still in water after a time period t is

$$f(t) = g_1(t) \cdot g_2(t) = g_1(t) \cdot \exp(-k_c t) \tag{1}$$

Eq. (1) is for a single O_2 molecule in the hydrated pore space. To scale it up to the soil sample with volume V and volumetric soil water content θ, we represent the number of dissolved O_2 molecules at the water-air interface in the soil sample at time t by $M(t)$. The number of dissolved O_2 molecules in the hydrated pore space at time t is hence

$$N(t) = \int_0^t M(\tau) g_1(t-\tau) e^{-k_c(t-\tau)} d\tau, \tag{2}$$

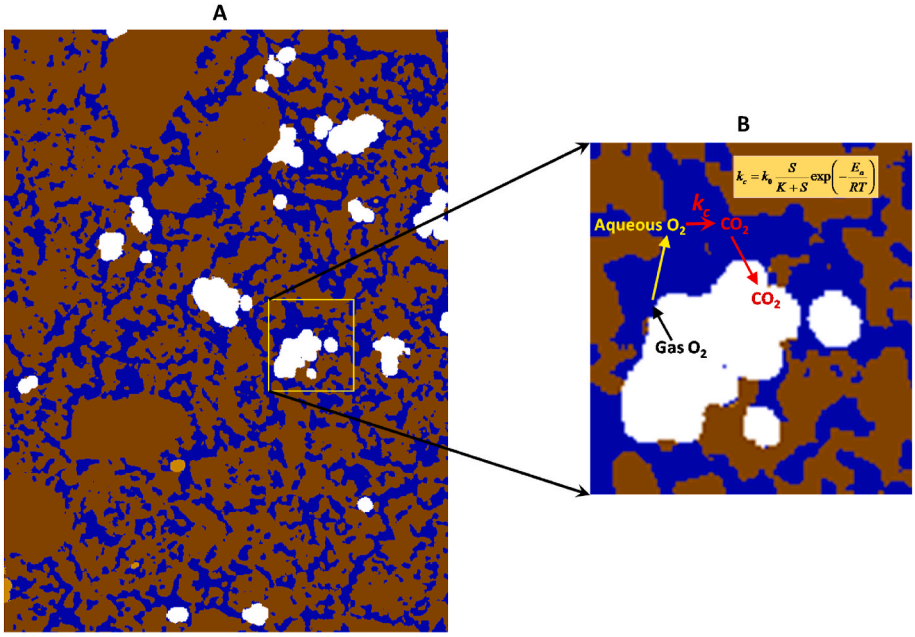

Fig. 1. (A) In the pore space with co-existence of water and air, (B) gaseous oxygen (O_2) dissolves at water (blue)-air (white) interface to become aqueous O_2. It then diffuses in the water. At microsites with the presence of microbes and substrates, aqueous O_2 is reduced. The reduction rate is k_c and depends on local temperature and substrate concentration. Microbial reduction of O_2 produces CO_2 which flows into the air-filled pores and then emits out of the soil.

The water-air interfacial areas in the soil sample are represented by $A_{wa}(\theta)$ when volumetric soil water content is θ, and the number of dissolved O_2 molecules on the water-air interface is proportional to $A_{wa}(\theta)$ and dissolved O_2 concentration on the water-air interface, $c_0(t)$, that is

$$M(t) = \xi \cdot A_{wa}(\theta) \cdot c_0(t), \tag{3}$$

where ξ is a parameter to balance the unit of both sides of Eq. (3). As microbial reduction of O_2 is a first-order kinetic, the respiration rate from the soil sample is hence

$$R_e(\theta, t) = \xi \cdot k_c \cdot A_{wa}(\theta) \cdot \int_0^t c_0(\tau) \cdot g_1(t-\tau) \cdot e^{-k_c(t-\tau)} d\tau, \tag{4}$$

The memory function $g_1(t)$ has been intensively studied in soil physics and subsurface hydrology (Coats and Smith, 1964; Haggerty and Gorelick, 1995; Chen and Wagenet, 1997; Hu et al., 2014; Zhang and Gao, 2016; Li et al., 2018). It can be directly calculated from soil structure (see Supplementary materials for details). To make the model analytical, it has been found that the following function, defined in its Laplace transform, can effectively describe the memory functions for different materials (Cvetkovic, 2012; Zhang and Gao, 2016):

$$G_1(s) = \int_0^\infty g_1(t) \cdot e^{-st} dt = \left[1 + \left(\frac{s}{a}\right)^b\right]^{-\beta}, \tag{5}$$

where s is the Laplace transform variable, and a, β and b are soil parameters which depend on soil structure and soil water content.

When $c_0(t)$ is a constant, O_2 movement and its microbial reduction in the soil sample reach equilibrium as time elapses. As proven in the Appendix, at equilibrium, the respiration rate from the soil sample is

$$R_0(\theta) = \xi \cdot k_c \cdot A_{wa}(\theta) \cdot c_0 \cdot \left[1 + \left(\frac{k_c}{a}\right)^b\right]^{-\beta}, \tag{6}$$

To reduce the number of parameters, we simplify Eq. (6) with β = b = 1. Physically, this is the same as the mobile-immobile model to describe the mass exchange between inter-aggregate and intra-aggregate pores (Coats and Smith, 1964; Haggerty and Gorelick, 1995), where $g_1(t) = a \cdot \exp(-at)$. This is a simplification but adequate to describe the impact of soil water on diffusion of dissolved O_2 (Haggerty and Gorelick, 1995). As demonstrated in the Supplementary materials, the parameter a is large when soil is dry and small when soil is wet. To reduce the number of parameters, we simplify the change in a with soil water content as follows (Hu et al., 2014):

$$a(\theta) = \frac{1}{a_1} \frac{\theta_s - \theta}{\theta}, \tag{7}$$

where θ_s is soil porosity and a_1 is a soil structure parameter.

The water-air interfacial area function $A_{wa}(\theta)$ is a soil structure parameter and varies with soil water content. Since $A_{wa}(\theta)$ is zero when soil is completely dried or fully saturated, $A_{wa}(\theta)$ is a "bell" shape function. For most soils we studied previously (Hu et al., 2014; Li et al., 2017) and the examples shown in the Supplementary materials (Figure S2), the change in $A_{wa}(\theta)$ with θ can be described by the following general function:

$$\begin{aligned} A_{ws}(\theta) &= A_0 \Theta^{b_1} (1-\Theta)^{b_2}, \\ \Theta &= \theta/\theta_s \end{aligned} \tag{8}$$

where Θ is saturation, and A_0, b_1 and b_2 are soil structure parameters.

2.2. Model for respiration from soil sample

From the mass balance, the mass of O_2 respired by microorganisms in a soil sample is balanced by the mass of O_2 dissolved at water-air interface in the soil when the system is at equilibrium. The O_2 dissolution at the water-air interface is a first-order kinetic (Zhang and Gao, 2016):

$$q = \kappa(C_{eq} - c_0) \tag{9}$$

where C_{eq} is the saturated dissolved O_2 concentration calculated from Henry's law, and κ is the dissolution rate coefficient. When soil water content is θ, the mass of O_2 dissolved at the water-air interface is the same as the mass of O_2 respired by microbes in the soil, that is,

$$\begin{aligned} &\kappa \cdot A_{wa}(\theta) \cdot (C_{eq} - c_0) = \xi \cdot k_c \cdot A_{wa}(\theta) \cdot c_0 \cdot E_r(\theta, k_c) \\ &E_r(\theta, k_c) = \left[1 + \left(\frac{k_c}{a(\theta)}\right)\right]^{-1} \end{aligned} \tag{10}$$

where the right-hand side in the first equation is equal to $R_0(\theta)$ in Eq. (6). Solving for c_0 gives

$$c_0 = \frac{\kappa \cdot C_{eq}}{\xi \cdot k_c \cdot E_r(\theta, k_c) + \kappa} \tag{11}$$

Substituting Eq. (11) into Eq. (6) yields

$$R_0(\theta) = k_c \cdot C_{eq} \cdot \xi \cdot A_{wa}(\theta) \left[\frac{1}{E_r(\theta, k_c)} + \frac{\xi \cdot k_c}{\kappa}\right]^{-1} \tag{12}$$

The first term inside the square bracket on the right-hand side represents the effect of O_2 diffusion in water and the second one is the impact of O_2 dissolution rate at the water-air interface. If O_2 dissolution rate is significantly faster than microbial reduction, that is, $\xi \cdot k_c/\kappa \to 0$, the second term in the square bracket reduces to zero. This is an assumption used in modelling oxygen reduction in hydrogen fuel cells (Sun et al., 2005; Zhang et al., 2014). As O_2 reduction in hydrogen fuel cells is far faster than microbial reduction of O_2 in soil, it is safe to assume $\xi \cdot k_c/\kappa \to 0$ for soils.

2.3. Moisture-temperature coupling and substrate accessibility

The parameter k_c in the above equations represents microbial reduction rate of O_2. It is a collective representation of other factors, including temperature, which affect microbial respiration. Its dependence on temperature is described by the Arrhenius equation (Davidson and Janssens, 2006):

$$k_c = \lambda(S) \exp\left(-\frac{E_a}{RT}\right) \tag{13}$$

where λ is the pre-exponential factor depending on substrate (represented by S) and substrate accessibility, E_a is the activation energy of the substrates, T is temperature and R is the gas constant. In comparison with experimental data in the next section, the substrates and other factors are collectively represented by the parameter λ.

Experimental observation revealed that substrates and their accessibility vary with pore sizes in that substrate accessibility in small pores is less than that in large pores (Bailey et al., 2017; Kravchenko et al., 2019a, 2019b). When soil water content is low, water and dissolved substrates are in small pores. Some of these pores, especially in clay-rich soils, might be smaller than microbes. Because of water viscosity and van der Waals force, substrates in these pores diffuse slowly and they are hence difficult for microbes to access. When soil water content is high, water and substrates are in both large and small pores and more accessible to microbes. To describe such pore-scale variations of substrate accessibility, we use water content as a proxy for pore size and allow λ to vary with soil saturation as follows:

$$\lambda = \lambda_0(S) \left[\Theta(\alpha_1 + \Theta)^{-1}\right]^{\gamma_1}, \tag{14}$$

where α_1 and γ_1 are parameters controlling the accessibility of substrates in different pores. Their respective impact on substrate accessibility is shown in the supplementary materials (Figure S4). For repacked sandy soils, where pores are large and substrates are spatially uniform over

pore space, the parameters α_1 and γ_1 are both zero.

2.4. Macropores

Some field and incubation experiments show significant CO_2 emissions even when soils approach saturation. Although some researchers have attributed this to denitrification and fermentation (Tang and Riley, 2019), the presence of macropores, such as cracks and bio-pores, also plays a critical role. These pores remain air-filled and provide pathways for atmospheric O_2 to enter the soil even when the surrounding matrix is saturated. Furthermore, even in incubation experiments where the macropores are eliminated, O_2 still dissolves at the soil surface and moves into soil water when soil is under fully saturated condition. To account for the effects of these factors, we modify the water-air interface function as follows, so that when soil matrix is saturated, there are still water-air interfaces for O_2 to dissolve and move into soil:

$$A_{wa}(\Theta) = A_0 \cdot \Theta^{b_1} (1 + \varepsilon - \Theta)^{b_2}, \tag{15}$$

where ε is a parameter representing the effects of macropores and the soil surface.

2.5. The model and comparison with experiments

The model for CO_2 emission from a soil sample is summarised as follows:

$$\begin{aligned} &R_0(\Theta, T) = k_c(T, \Theta) \cdot A(\Theta) \cdot C_{eq} \cdot E_r(\Theta, T), \\ &A(\Theta) = \xi \cdot A_0 \cdot \Theta^{b_1} (1 + \varepsilon - \Theta)^{b_2}, \\ &E_r(\Theta, T) = \left[1 + a_1 \cdot k_c \frac{\Theta}{1 - \Theta}\right]^{-1}, \\ &k_c(T, \Theta) = \lambda_0(S) \left[\Theta(\alpha_1 + \Theta)^{-1}\right]^{\gamma_1} \exp\left(-\frac{E_a}{RT}\right), \end{aligned} \tag{16}$$

Eq. (16) demonstrates that the influence of temperature, soil water content and other factors (represented by λ_0) on soil respiration are nonlinearly integrated in that a change in one of them will affect the response of soil respiration to the change in others. This paper assumed substrate is not a limiting factor and $\lambda_0(S)$ in each example is constant.

The model involves a number of parameters, each having its physical interpretations as explained above. Since ξ, A_0, a_1 are soil parameters and are constants for a given soil, to reduce the number of parameters, we combine them by rewriting Eq. (16) as follows:

$$\begin{aligned} &R_0(\Theta, T) = k'(T, \Theta) \cdot A'(\Theta) \cdot C_{eq} \cdot E_r(\Theta, T), \\ &A'(\Theta) = \Theta^{b_1} (1 + \varepsilon - \Theta)^{b_2}, \\ &E_r(\Theta, T) = \left[1 + a' \cdot k' \frac{\Theta}{1 - \Theta}\right]^{-1}, \\ &k'(T, \Theta) = \lambda'(S, T) \left[\Theta(\alpha_1 + \Theta)^{-1}\right]^{\gamma_1}, \\ &\lambda'(S, T) = \xi \cdot A_0 \cdot \lambda_0(S) \cdot \exp\left(-E_a \cdot R^{-1} \cdot T^{-1}\right);\ a' = a_1 \cdot \xi^{-1} \cdot A_0^{-1}. \end{aligned} \tag{17}$$

We use the law of scaling to compare the model and experiments in that a scaled respiration calculated from Eq. (18) is the same as the experimental respiration scaled by the same method (Ebrahimi and Or, 2016). For experiments that have only moisture gradient and the temperature is constant (represented by T_0), the law of scaling is

$$R'(\Theta, T_0) = \frac{\left[\Theta(\alpha_1 + \Theta)^{-1}\right]^{\gamma_1} \cdot A'(\Theta) \cdot E_r(\Theta, T_0)}{\left[\Theta^*(\alpha_1 + \Theta^*)^{-1}\right]^{\gamma_1} \cdot A'(\Theta^*) \cdot E_r(\Theta^*, T_0)} \approx \frac{R_E(\Theta, T_0)}{\Omega(\Theta^*, T_0)}, \tag{18}$$

where Θ^* is the saturation at which $\left[\Theta(\alpha_1 + \Theta)^{-1}\right]^{\gamma_1} \cdot A'(\Theta) \cdot E_r(\Theta, T)$ peaks, $R_E(\Theta, T_0)$ is the measured respiraitonin in experimemnts, and $\Omega(\Theta^*, T_0)$ is the respiration when the saturation is Θ^* in the experiments. Depending on the experiments, we either directly compared the scaled respiration calculated from Eq. (18) with experimental data, or multiplied the scaled respiration calculated from Eq. (18) by the scalar $\Omega(\Theta^*, T_0)$, to account for the size effect in the experiments, i.e., $R_E(\Theta, T_0) = \Omega(\Theta^*, T_0) \cdot R'(\Theta, T_0)$. There are seven parameters in Eq. (18): α_1, γ_1, b_1, b_2, ε, a' and $\lambda(S,T_0)$. To reduce the number of parameters, b_1 and b_2 were assumed to be the same in all experiments; their values are the averages of the results we calculated for different soil samples. This is an approximation but captures the change in water-air interfacial area with soil water content, as well as its impact on respiration.

In the experiment with both temperature and moisture gradients, we first used the data measured from different soil water contents and under the same temperature (represented by T_0) to estimate the soil structure parameters and the scalar $\Omega(T_0)$ using Eq. (18) and the procedures discussed above. We then predicted the change in respiration with temperature without introducing extra parameters. From Eq. (17), the parameter $\lambda'(\Theta, T)$ associated with temperature T is calculated from $\lambda'(\Theta, T) = \exp[E_a R^{-1}(T_0^{-1} - T^{-1})] \cdot \lambda'(\Theta, T_0)$; the value of E_a took the value recommended in the literature (Davidson, 2020); to account for the change of O_2 dissolution with temperature, the scalar factor associated with temperature T is calculated from $\Omega(T) = \Omega(T_0) C_{eq}(T) / C_{eq}(T_0)$ because the respiration is proportional to C_{eq} (Eq. (16)), where $C_{eq}(T)$ and $C_{eq}(T_0)$ are the values of C_{eq} at temperature T and T_0 respectively.

The functions in Eq. (18) are simple and we used the curve fitting toolbox in the Matlab to fit the model to the experimental data.

3. Results

3.1. Impact of substrate heterogeneity and macropores

The impact of substrate heterogeneity and soil structure on soil respiration is represented by several characteristic parameters. Although the variation in water-air interfacial areas with soil water content is a soil structure parameter, herein we focus on pore-scale substrate heterogeneity and macropores. To emphasise the importance of these soil parameters in influencing the moisture-respiration relationship, the temperature and substrate parameters are not limiting factors, that is, the parameter $\lambda'(S, T)$ in Eq. (17) is constant. The moisture sensitivity is calculated from Eq. (18), which is equivalent to the moisture functions used in SOC models (Bauer et al., 2008). The two parameters characterising water-air interfacial areas took $b_1 = 1.3$ and $b_2 = 0.8$ in all examples. This is an approximation but rational as it captures the change in water-air interfacial areas with soil water.

We first demonstrate the effect of the two parameters, α_1 and γ_1, characterising the pore-scale substrate heterogeneity; their impact on pore-scale substrate is shown in Fig. S4. When $\alpha_1 = 0$, λ is a constant and the substrate accessibility is independent of pore size and is spatially uniform. With γ_1 increasing, substrate accessibility in small pores decreases faster while those in large pores increases faster. Fig. 2A shows the change in the moisture-respiration relationship when α_1 is changed from 0.2 to 20 with other parameters kept the same. With α_1 increasing, the accessibility of substrates in small pores decreases and those in larges increases. As a result, respiration from small pores decreases while that from large pores increases, the moisture-respiration curve shifts to the right. Fig. 2B shows the change in the moisture-respiration relationship when the parameter γ_1 is increased from 0.5 to 3.0 with other parameters remaining the same. As shown in Fig. S4, with γ_1 increasing, the increase in substrate accessibility with pore size changes from "concave-down" increase (when $\gamma_1 < 1$) to "concave-up" increase (when $\gamma_1 < 1$). As a result, with γ_1 increasing, the increase in the respiration with soil water becomes increasingly "concave-up" at the dry end, and the moisture-respiration curve shifts to the right. Fig. 2C shows the impact of macropores on the moisture-respiration relationship when other parameters are the same. Increasing macropores means that O_2 still dissolves and moves into the water when the matrix is fully saturated. Therefore, increasing macroporosity affects the respiration on the wet end more profoundly than on the dry end.

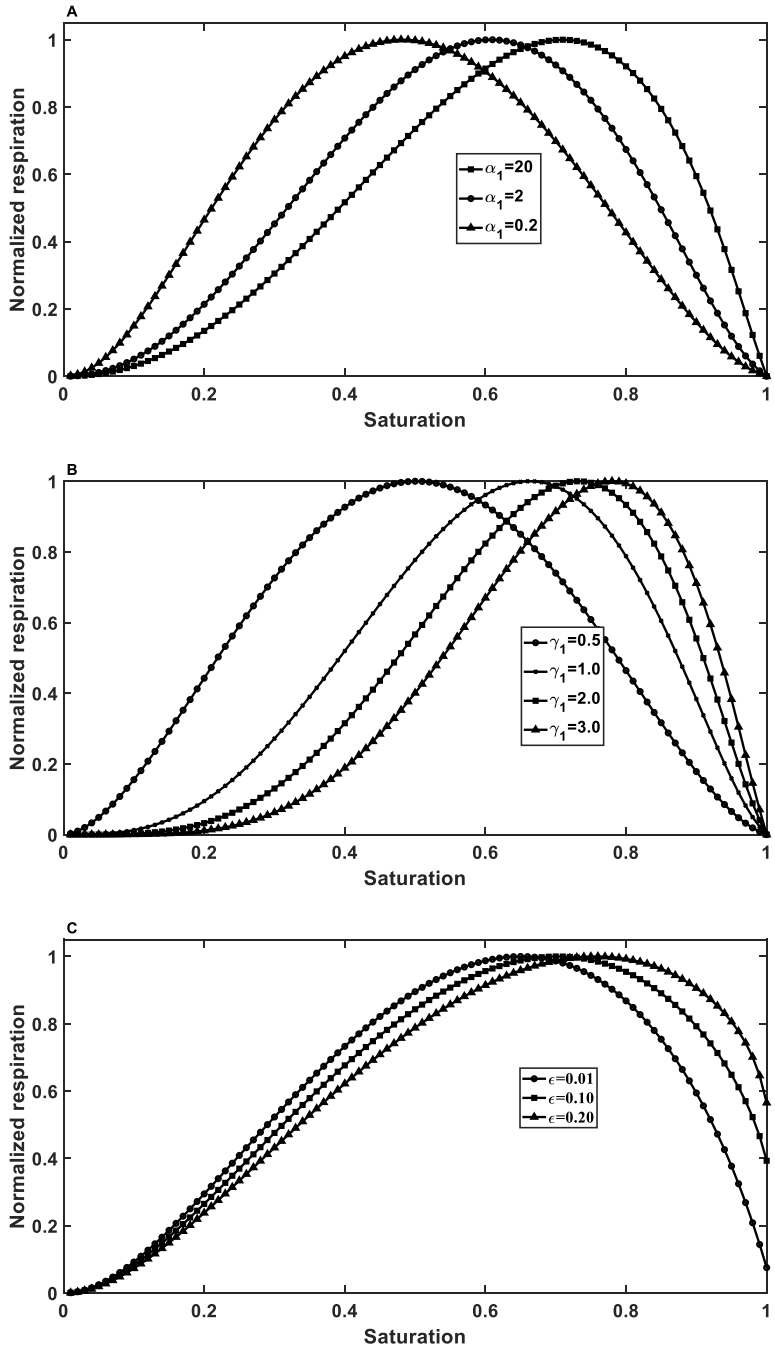

Fig. 2. Effect of pore-scale substrate accessibility on the moisture response of the respiration. (A) Effect of the parameter α_1 which controls substrate heterogeneity ($\xi A_0 = 1.0$, $\lambda_0 \exp(-E_a/RT) = 1.0$, $\varepsilon = 0$, $\alpha_0 = 1.0$, $\gamma_1 = 1.0$). (B) Effect of the parameter γ_1 which controls the skewness of the pore-scale substrate distribution ($\xi A_0 = 1$, $\lambda_0 \exp(-E_a/RT) = 1$, $\varepsilon = 0$, $\alpha_0 = 1.0$, $\alpha_1 = 1.0$). (C) Effect of the porosity of macropore ε ($\xi A_0 = 1$, $\lambda_0 \exp(-E_a/RT) = 0.01$, $\alpha_0 = 1.0$, $\gamma_1 = 1.0$, $\alpha_1 = 0.1$).

3.2. Comparison with experimental data

We compare the model with five experiments, four with moisture gradient only and one with both temperature and moisture gradients. We use these examples to demonstrate: i) the model captures the fundamental mechanisms governing the response of respiration to soil water change, ii) temperature and soil water are nonlinearly coupled in their influence on soil respiration, iii) the model correctly describes this nonlinear integration. The change in respiration with soil water and temperature is mediated by various factors and for each example, we made rational simplifications (described in each experiment) in order to reduce the number of parameters. The values of the parameters and the associated Akaike Information Criterion (AIC) for each experiment are given in Table 1.

3.2.1. Moisture response

There was no temperature gradient in these examples and the parameter $\lambda'(T, S)$ in Eq. (17) is hence constant. The respiration in all examples is calculated by Eq. (18), with the calculated results converted or not converted to real respiration (see details for each example).

The first example is an incubation experiment using a sandy soil (Skopp et al., 1990), where the respiration rates measured at different soil water contents were normalized by the maximum respiration rate at the optimal moisture content. Sieving helped homogenise the substrates,

Table 1
Parameters and their values for each of the five experimental examples we compared. The symbol "-" means that the associated parameter was zero and not calibrated in the comparison. The parameters b_1 and b_2 are the same for all examples.

Parameter	Example				
	1	2	3	4	5
b_1	1.3*	1.3*	1.3*	1.3*	1.3*
b_2	0.8*	0.8*	0.8*	0.8*	0.8*
a_1 (s)	0.9	10.0	0.06	0.02	0.3
ε	–	–	0.65	0.25	0.08
λ_0 (s^{-1})	0.3	2.3	0.04	5.0	2.8
α_1	–	1.0	0.15	0.2	1.2
γ_1	–	4.3	0.51	1.31	1.1
Ω	–	–	0.015 (μg g^{-1} s^{-1})	5.5 (μg m^{-2} s^{-1})	1.8 (μg g^{-1} h^{-1})
AIC	−21.6	7.11	−102	35.1	8.08

and we hence assume pore-scale substrate distribution is uniform with the parameters α_1 and γ_1 in Eq. (14) being zero. Also, macropores were unlikely to develop in repacked sandy soil and the parameter ε in Eq. (13) is zero. Therefore, there are only two parameters, $\lambda'(T, S)$ and a', We adjusted them to fit the experimental data; the modelled results and the experimental data are compared in Fig. 3A; they agree well with $R^2 = 0.91$ and $p = 1.3 \times 10^{-7}$.

The second example is also an incubation experiment using a silty clay loam (Linn and Doran, 1984), where CO_2 production was measured when soil saturation was increased from 10% to 95%. We adjusted the values of other parameters to reproduce the measured data; the modelled and measured respiration rates (normalized) are compared in Fig. 3B. The model captures the variation in respiration well when soil water content is lower than the optimum, but there is a discrepancy between them when soil water content exceeds the optimum. Overall, they agree reasonably well with $R^2 = 0.75$ and $p = 0.0026$.

The third example is an incubation experiment using an undisturbed luvisol soil (Herbst et al., 2016), where the respiration rate increased approximately linearly with soil water content. The driver behind this moisture-respiration relationship is likely due to the presence of macropores, because the undisturbed luvisol is a structured soil and the pore-scale substrate distribution in it is likely to be heterogeneous. The increase in respiration with soil water content at the dry end is concave-downward, meaning that the value of the parameter γ_1 in Eq. (14) is less than 1 as demonstrated in Fig. 3C. We reproduced the experimental data by adjusting these parameters, and the comparison between the measured and calculated respiration rates is shown in Fig. 3C. They agree well with $R^2 = 0.94$ and $p = 1.3 \times 10^{-6}$.

The fourth example is respiration measured under different soil water contents from a loamy soil at an oak savanna field site (Curiel Yuste et al., 2007). Macropores due to fauna and root activity were likely to have developed in such fields, manifested by the continuous increase in respiration when the soil approached saturation (Curiel Yuste et al., 2007). Also, substrates and microbial communities are likely to vary with pore sizes in undisturbed field soil. Incorporating these processes needs more parameters, but it can reproduce the response of respiration to soil moisture change more accurately as shown in Fig. 3D ($R^2 = 0.88$ and $p = 1.9 \times 10^{-5}$), especially at the dry end where the model correctly captures the sigmoid-type increase in respiration as soil water content increases.

3.2.2. Moisture-temperature coupling

The last example is an incubation experiment with both moisture and temperature gradients (Zhou et al., 2014). We first estimated the soil-structure parameters based on the respiration rates measured from different saturations under temperature 31 °C, and then predicted the change in respiration as temperature was increased. Based on Davidson (2020), the activation energy of substrates in the soil took $E_a = 55$ kJ

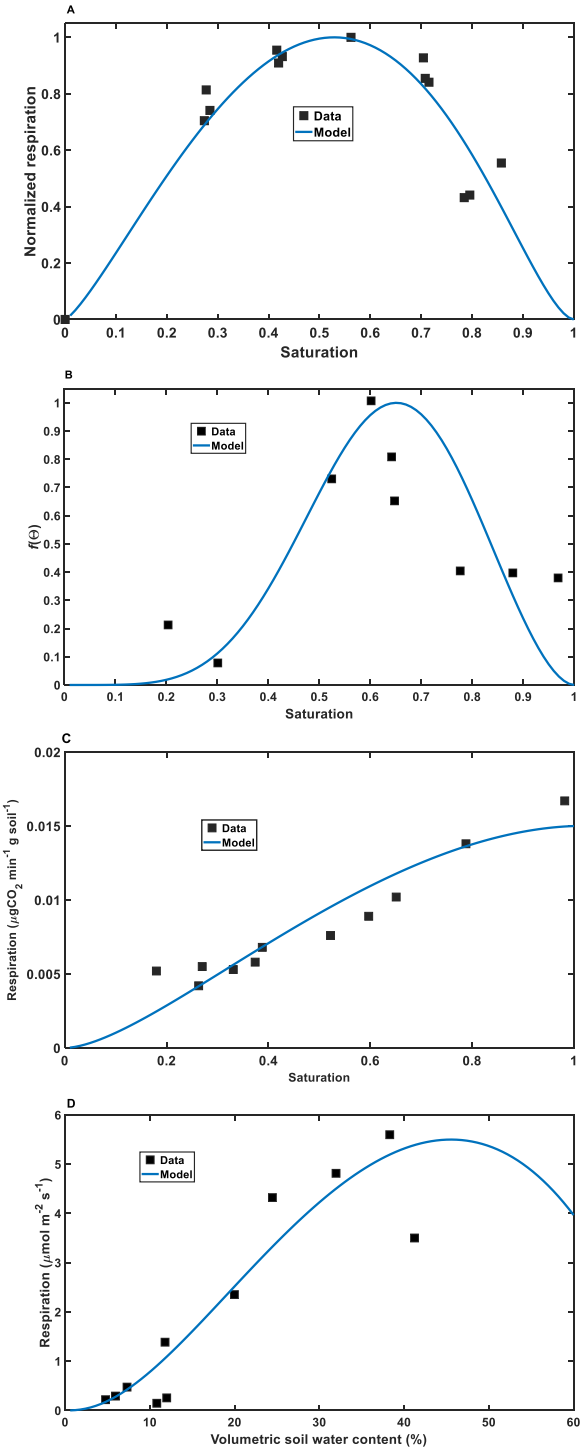

Fig. 3. Comparison between calculated respiration rates under different soil saturations with those measured from various experiments. (A) Incubation using a sieved sandy soil (Skopp et al., 1990); (B) incubation using a sieved silty clay loam; (C) incubation using an undisturbed luvisol soil (Herbst et al., 2016); (D) a field experiment on a loamy soil at an oak savanna site (Curiel Yuste et al., 2007).

mol^{-1}. Also, the soil was sieved and mixed; pore-scale substrate distribution was hence assumed to be uniform (α_1 and γ_1 in Eq. (18) were both zero) and the porosity of macropores was zero. We calibrated other parameters to reproduce the respiration rates measured under different saturations at 31 °C; the modelled and measured respiration rates are compared in Fig. 4A ($R^2 = 0.93$ and $p = 0.009$).

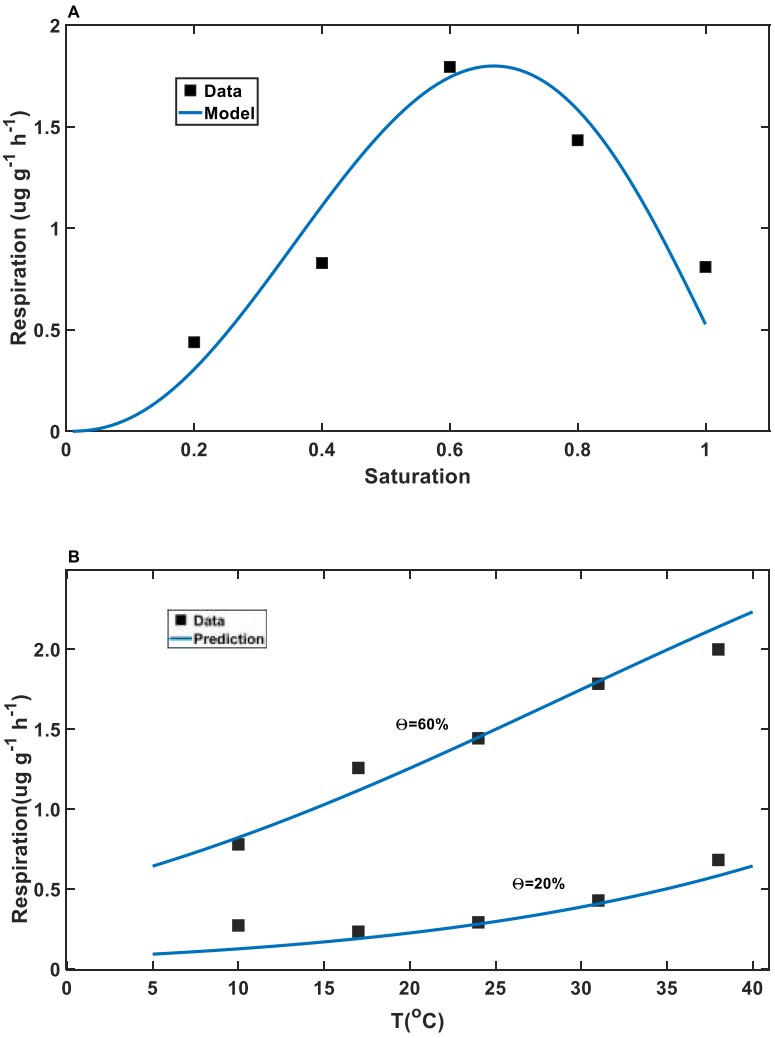

Fig. 4. (A) Comparison between measured and modelled respiration rates at different soil saturations under 31 °C for a sandy soil using E_a = 55 kJ mol^{-1}. (B) Comparison between the measured and predicted respiration rates when the temperature was increased from 10 to 38 °C at saturation of 20 and 60%, respectively.

Using these soil structure parameters and the estimated parameter λ'(T, S) at 31 °C, we predicted the change in respiration when temperature was increased from 10 to 38 °C with soil saturation kept at 20 or 60%, respectively. Fig. 4B compares the predicted and measured change in respiration rates when temperature was increased from 10 to 38 °C. It is manifest that the model predicts the increase in respiration with temperature reasonably well at both saturations, with R^2 and p of the prediction being 0.88 and 0.018 for saturation 20%, and 0.98 and 0.002 for saturation 60%, respectively.

4. Discussion

In unsaturated soils, O_2 is the main electron acceptor for microbial respiration. Although O_2 had been included as a limiting factor previously to model respiration measured from incubation experiments with controlled O_2 supply (Davidson et al., 2012; Sierra et al., 2017; Azizi-Rad et al., 2022), in soils, bioavailable O_2 is not an independent variable but mediated by soil water as atmospheric O_2 must dissolve at the water-air interface and diffuse into the regions proximal to microbes first before becoming bioavailable. Therefore, soil water and bioavailable O_2 cannot be represented as two independent variables. Furthermore, bioavailable O_2 is also affected by temperature in different ways. Physically, increasing temperature reduces O_2 dissolution at water-air interface. Biologically, increasing temperature boosts microbial activity at the reactive sites and increases their demand for O_2; this depletes O_2 in the proximity of the microbes and steepens the concentration gradient between water-air interface and the microbes. These processes occur in hydrated pore space but regulate the moisture response of respiration from soil samples (Chakrawal et al., 2020; Wilson and Gerber, 2021). Eq. (16) indicates that all factors which influence microbial reduction of O_2 are nonlinearly integrated in their impacts on soil respiration. Microbial respiration involves a myriad of interdependent biotic and biotic processes and its modelling for large scale needs to be parsimonious. To make the model analytical, we approximate microbial reduction of O_2 at reactive sites in the hydrated pore spaces as a first-order kinetic process. However, this differs from the first-order kinetic models used by others (Fang and Moncrieff, 2001), which use bulk soil properties. In the proposed model, though microbial reduction of O_2 at microsites is a first-order kinetic process, summing all microsites in a soil sample makes the total respiration from the soil no longer proportional to the kinetic reaction rate (Eq. (16) and Eq. (17)).

4.1. Improvement of the proposed model

Most SOC models use a soil moisture function to describe the moisture effect (Liu et al., 2009; Moyano et al., 2013; Manzoni et al., 2016; Bailey et al., 2019; Liang et al., 2022). Although the moisture functions used by different models vary, they use one or two soil water contents to

cut the moisture-respiration curve into two or three portions (Skopp et al., 1990; Bauer et al., 2008; Yan et al., 2018). The experimental data, however, do not show existence of such cut-offs (Figs. 2 and 3). Considering that the diffusion coefficient of gaseous O_2 is in the order of 10^{-1}(cm^2 s^{-1}), while the diffusion coefficient of dissolved O_2 is in the order of 10^{-5} (cm^2 s^{-1}). We hence argue that it is the dissolution and diffusion of O_2 in water, both varying with soil water content, that control the response of respiration to soil water content change. Our model is developed from this principle, and it captures the smooth and diverse variation of respiration with soil water content.

A critical issue in moisture functions currently in use is that they do not account for the variation of substrate over pore space and macropores, which impact the moisture response of respiration (Franklin et al., 2021; Zheng et al., 2022). We include these and demonstrate that a small change in them could lead to a substantial shift in the moisture-respiration relationship (Fig. 2). It is worth to point out that the parabolic function is often used as an empirical model to describe the moisture effect (Zheng et al., 2022), and our results show that this appears to apply to sieved sandy soils where substrate distribution is homogenised and macropores are destroyed (Fig. 3A and B, Fig. 4A); it is not appropriate for field or intact soils where pore-scale substrate distribution is heterogeneous and macropores exist (Fig. 3C and D). Also, Reichstein et al. (2003) used a Michaelis-Menten type function to describe the moisture-respiration data measured from 17

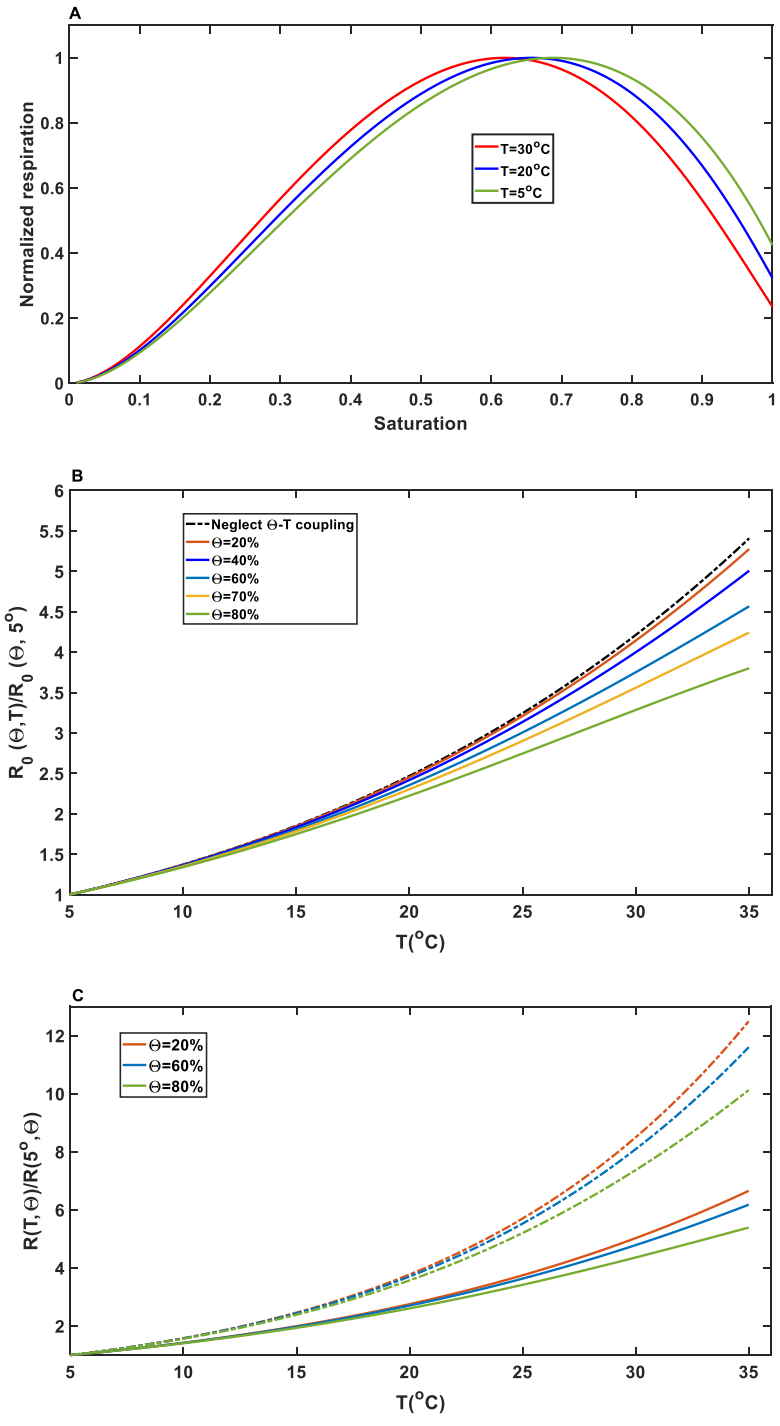

Fig. 5. (A) Change in the moisture-respiration (normalized by the maximum respiration rate) relationship when temperature is increased from 5 to 30 °C, with other parameters being the same. (B) The impact of soil saturation on the temperature sensitivity of the respiration (for each Θ, the respiration rate at temperature T, R_0(Θ, T), is normalized by the respiration rate at 5 °C). (C) Comparison of the temperature sensitivity of the respiration calculated with (solid lines) and without (broken lines) considering the temperature-dependent O_2 dissolution.

different forest and shrubland sites in Europe and North America, which is similar to Figs. 2C and 3C, whose underlying mechanisms are substrate heterogeneity and macropores. As our model can produce the diverse moisture-respiration relationships measured from various experiments, it captures the key mechanisms governing the response of respiration to soil water change.

4.2. Moisture-temperature coupling and its implications

We chose to work on O_2 because the factors and processes which affect the bioavailability of O_2 are physical and their mechanistic modelling has been well established in other areas (Zhang and Gao, 2016; Li et al., 2018). This enables us to differentiate the physical processes and microbial activities. We show that soil water, temperature and other factors are nonlinearly integrated in their impact on respiration from soil samples. The close agreement between the measured and modelled variations of the respiration with temperature and soil water indicates that they are indeed nonlinearly interconnected in their influence on the respiration (Fig. 4).

The nonlinear coupling between soil water and temperature means that a change in one affects the response of the respiration to the other one, and that their combined effect is not multiplicative as commonly presumed in most SOC models (Falloon et al., 2011; Li et al., 2023). This could be partly responsible for the variation in the predicted response of SOC to temperature rise when using different moisture functions (Falloon et al., 2011; Sierra et al., 2015). To demonstrate the implications of moisture-temperature coupling, Fig. 5A shows the change in the moisture-respiration relationship calculated using Eq. (18) when temperature is increased from 5 to 30 °C when other soil structure and substrate parameters are the same. The increased microbial metabolism due to temperature rise boosts microbial consumption of O_2, thereby reducing the O_2 concentration in the regions proximal to microbes and making the regions more anoxic. As a result, the optimal moisture content for aerobic microbes shifts to the left. Equally, a change in soil water content also affects the response of the respiration to temperature rise; Fig. 5B shows that the temperature sensitivity of the respiration decreases as soil saturation increases because of the increased attenuation on diffusion of dissolved O_2. This is consistent with the general view that SOC in tropical regions (characterised by high rainfall and hence high soil water content) is less sensitive to warming (Davidson, 2020). Haff et al. (2021) showed that, globally, Q_{10} in the latitude from 40°S to 40°N is significantly lower than that in other regions. While there are other biotic and abiotic mechanisms behind this phenomenon, moisture-temperature coupling might also play a role, as it attenuates the temperature sensitivity of the respiration, with the attenuation increasing with temperature (Zhang et al., 2022). Another mechanism is O_2 dissolution, which decreases with temperature rising (Figure S5). Fig. 5C shows that not considering the temperature-dependent O_2 dissolution exaggerates the temperature sensitivity of the respiration, and that the exaggeration increases with temperature.

4.3. Oxygen diffusion and substrate accessibility

Microbial respiration in unsaturated soils is modulated by O_2 and substrate accessibility. After its dissolution at the water-air interface, O_2 movement is controlled by its molecular diffusion coefficient and distribution of water in the pore space (Fig. 1). Their combined effect is represented by the parameter a_1 in Eq. (7). The unit of a_1 is time, and a_1 is related to molecular diffusion coefficient of dissolved O_2 (D) and a length parameter (τ) which characterises the average distance between water-air interface and where the microbes reside (Fig. 1); their relationship is $a_1 \propto \tau^2/D$ (Hu et al., 2014). Previous work showed that τ depends on soil texture and that its value for repacked rounded sands is smaller than that for aggregated soils (Coats and Smith, 1964; Haggerty and Gorelick, 1995; Zoia et al., 2010; Hu et al., 2014; Li et al., 2017). Clay is an important factor in soil aggregation and is often used as a soil texture indicator in some SOC models (Tang and Riley, 2019; Zheng et al., 2022). It is hence rational to assume that a_1 increases with clay content (S_c) in $a_1 = \eta_0 S_c/(K_c + S_c)$, or $a_1 = \eta_0 S_c^{'}/(1 + S_c^{'})$, where $S_c^{'} = S_c/K_c$, and η_0 and K_c are parameters. That is, increasing clay content creates more small pores and small aggregates, thereby increasing the distance between water-air interface and wetted pore walls (Figure S6).

The increase in small pores due to the increase in clay content makes substrates in them less accessible, as microbes can only access, directly, substrates in the pores that the microbes can get through. This increases the pore-scale heterogeneity of bioavailable substrates. In the meantime, increasing clay content enhances soil aggregation and formation of macropores (Beven and Germann, 2013; Bacq-Labreuil et al., 2018). We can modify the parameters in Eqs. (14) and (15) as follows $\alpha_1 = \alpha_0 S_c/(K_c + S_c)$, $\gamma_1 = \gamma_0 S_c/(K_c + S_c)$ and $\varepsilon = \varepsilon_0 S_c/(K_c + S_c)$ to account for the effects of clay content on these processes: with the increase in clay content, α_1 and γ_1 increase and substrates in small pores become increasingly less accessible compared to substrates in large pores (Figure S4). Fig. 6A demonstrates how an increase in relative clay content (S_c/K_c) shifts the moisture-respiration curve towards to the right. This is consistent with the theoretical analysis (Yan et al., 2016; Tang and Riley, 2019; Zheng et al., 2022) and experimental results (Franzluebbers, 1999). Interestingly, because of its nonlinear coupling with temperature (Eq. (16)), Fig. 6B shows that a change in clay content also affects the temperature response of the respiration.

4.4. Importance to distinguish between physical factors and biological factors

Microbial respiration is complex, influenced by many biotic and abiotic factors. Different factors might have similar effects on the changes in respiration with soil water and/or temperature. Previous work had attributed these changes as biological consequences such as microbial adaptation (Hawkes et al., 2017). Microbial adaptation does exist, but our studies demonstrate the importance of physical factors which have been neglected. For example, the presence of a small fraction of macropores can significantly change the moisture response of respiration at the wet end (Figs. 2C and 3C, D). In the field, especially in fine textured soils, periodic drying-rewetting is common, which results in soil cracking (Beven and Germann, 2013). In fact, de Nijs et al. (2019) indeed found that repeated drying-wetting changed the moisture-respiration relationship. Though the authors attributed this change as a consequence of microbial processes (de Nijs et al., 2019), herein we show that change in soil structure could lead to the same phenomena. In another example, Hawkes et al. (2017) studied the variation in moisture-respiration relationship over a region with precipitation gradient; they found that, in the dry end, the respiration increased with soil water content in a concave-upward way for clay-rich soils, while for clay-poor soils, the increase was concave-down. Again, the authors attributed such respiration variations with soil texture as a consequence of microbial adaptation; our analysis shows that the reduced accessibility of substrates in small pores due to the increased clay content in clay-rich soils can also give rise to such phenomena (Fig. 6A). Microbial adaptation is important, but physical factors and processes are also crucial. Neglecting them in data analysis would result in their effects being mistaken for microbial adaptation, thereby overestimating the role of microbial acclimation in predicting the response of SOC to warming.

Similar to the microbial dimension as addressed recently by Schimel (2023), soil structure and physical processes are equally important and should be included in modelling ecosystem carbon dynamics. Including them inevitably increases the number of parameters, but this is a price probably worth paying in order to improve the predictability of SOC models. Future work should focus on reducing the number of parameters without compromising the representation of soil-structure and physical

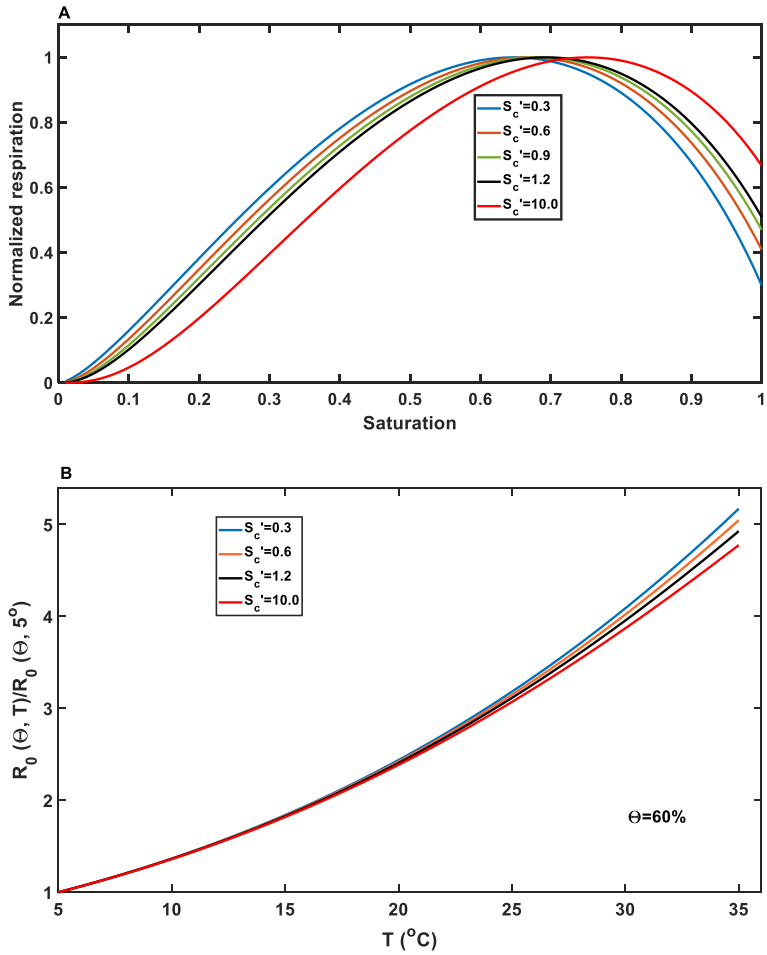

Fig. 6. Increasing clay content shifts the moisture-respiration curve towards the wet end due to the increased small pores in which substrates are less accessible to microbes (A). Change in clay content also alters the temperature sensitivity of the respiration (B).

processes in SOC models. For the model we developed, the water-air interfacial parameters can be directly measured (Faisal Anwar et al., 2000). For ecosystem modelling, however, these parameters need to be estimated using easy-to-measure soil properties via pedo-transfer functions.

4.5. Potential link to soil organic carbon modelling

Our primary purpose is to propose a new concept to model the moisture and temperature response of the respiration. We hence simplified the microbes and substrates by describing them collectively using a single parameter λ (Eqs. (13) and (14)). The concept, however, can be used to model SOC dynamics as microbial reduction of O_2 at each microsite depends on cell numbers and substrate abundance. For example, if the substrate effect is described by the Michaelis-Menten equation (Davidson et al., 2012), and microbial reduction of O_2 is proportional to cell numbers (Tang and Riley, 2019), the kinetic rate k_c in Eq. (16) can be modified to account for the substrates and microbes:

$$k_c = \eta_0 \cdot n \cdot \frac{S}{K_S + S} \cdot \left[\Theta(\alpha_1 + \Theta)^{-1}\right]^{\gamma_1} \exp\left(-\frac{E_a}{RT}\right) \tag{19}$$

where n and S are average cell numbers and substrate abundance at each reactive site, respectively, and K_S is the affinity parameter for the substrates. Because of the nonlinearity of Eq. (17), changes in cell numbers and substrate abundance also affect the moisture and temperature response of the respiration. We do not delve into this further as the focus of this paper is to present the new conceptual model and its implications.

5. Conclusion

We propose a new concept to model the moisture effect of the heterotrophic soil respiration by tracking dissolution, diffusion, and microbial reduction of O_2 in hydrated reactive sites, and then summing the reduction of all O_2 in a soil sample. The model for calculating total respiration from the soil sample was derived based on mass balance that the mass of O_2 dissolved at the water-air interface in the soil sample is the same as the mass of O_2 reduced by microbes in the soil. This allows us to include explicitly pore-scale substrate heterogeneity, macropores, temperature and other factors. Comparison with experimental data shows that the model can reproduce the diverse moisture-respiration relationships measured from various experiments, and that soil parameters calibrated from one temperature can predict the variation of the respiration after temperature changes. We also show that soil moisture, temperature, and clay content are nonlinearly integrated in their impacts on soil respiration, and that a change in one of them alters the response of the respiration to the changes in others. In particular, we find that for a given substrate, the temperature response of microbial respiration is not constant but varies with soil water content and soil texture. Also, for a given soil, its moisture effect on heterotrophic respiration is not a single function but varies with other factors. All these suggest that developing SOC models in the future should consider these physical processes.

Declaration of competing interest

The authors declare the following financial interests/personal relationships which may be considered as potential competing interests: Zhongdong Huang reports financial support was provided by National Key R&D Program of China. Yuan Liu reports financial support was provided by National Key R&D Program of China. Yuan Liu reports financial support was provided by Central Public-interest Scientific Institution Basal Research Fund. Zhongyang Li reports financial support was provided by National Key R&D Program of China. Zhongyang Li reports financial support was provided by Central Public-interest Scientific Institution Basal Research Fund. Xiaoxian Zhang reports financial support was provided by Biotechnology and Biological Sciences Research Council. Xiaoxian Zhang reports was provided by Natural Environmental Research Council (NERC) of the UK.

Data availability

No data was used for the research described in the article.

Acknowledgements

This work was funded by the National Key R&D Program of China (2022YFF0711800, 2021YFD1700900), the Central Public-interest Scientific Institution Basal Research Fund (FIRI2022-04 and Y2022LM29). The work at Rothamsted is funded by the Biotechnology and Biological Sciences Research Council of the UK through the strategic programmes of Growing Health (BBS/E/C/00010310) and Delivering Sustainable Wheat (BB/X011003/1); it is also funded by the Natural Environmental Research Council of the UK (NE/T010487/1).

Appendix

The Laplace transform of a function $f(t)$ is defined by

$$F(s) = \int_0^\infty f(t)\exp\left(-st\right)dt, \tag{A1}$$

Applying the Laplace transform to Eq. (4) and using the convolution theorem, we have

$$\overline{R}_e(\theta, s) = \xi \cdot k_c \cdot A_{wa}(\theta)\cdot\overline{C}_0(s)\cdot\overline{G}_1(s+k_c) \tag{A2}$$

where

$$\overline{R}_e(\theta, s) = \int_0^\infty R_e(\theta, t)\exp(-st)dt, \quad \overline{C_0}(s) = \int_0^\infty c_0(t)\exp(-st)dt, \overline{G_1}(s) = \int_0^\infty g_1(t)\exp(-st)dt, \tag{A3}$$

When $c_0(t)$ is a constant, $\overline{C_0}(s) = c_0/s$. From Eq. (5) we thus have

$$\overline{R}_e(\theta, s) = \xi \cdot k_c \cdot A_{wa}(\theta)\cdot c_0\frac{1}{s}\left[1 + \left(\frac{s+k_c}{a}\right)^b\right]^{-\beta}, \tag{A4}$$

The system reaches a state of equilibrium as time elapses. At steady state, the respiration from a soil sample is calculated as follows:

$$\begin{aligned} R_0(\theta) = \underset{t\to\infty}{R_e}(\theta, t) &= \underset{s\to 0}{L^{-1}}[R_e(\theta, s)] = \underset{s\to 0}{L^{-1}}\left\{\xi \cdot k_c \cdot A_{wa}(\theta)\cdot c_0\frac{1}{s}\left[1 + \left(\frac{s+k_c}{a}\right)^b\right]^{-\beta}\right\} \\ &= \xi \cdot k_c \cdot A_{wa}(\theta)\cdot c_0 \cdot \left[1 + \left(\frac{k_c}{a}\right)^b\right]^{-\beta} \underset{s\to 0}{L^{-1}}\left(\frac{1}{s}\right) \\ &= \xi \cdot k_c \cdot A_{wa}(\theta)\cdot c_0 \cdot \left[1 + \left(\frac{k_c}{a}\right)^b\right]^{-\beta} \end{aligned} \tag{A5}$$

where $\underset{s\to 0}{L^{-1}}[\overline{R}(s)]$ represents taking inverse Laplace transform of $\overline{R}(s)$ when $s\to 0$.

Nomenclature

$g_1(t)$ Memory function: probability of a O_2 molecule remaining in water at time t following its dissolution when there are no any biochemical reactions
k_c (s^{-1}) Kinetic reaction rate for the first-order microbial reduction of O_2 at microsites
N(t) (mg) Mass of dissolved O_2 in hydrated pore space in a soil sample at time t
A_{wa} (θ) (cm^2) Water-air interfacial area in a soil sample when soil water content is θ
θ Volumetric soil water content
c_0(t) (mg L^{-1}) Dissolved O_2 concentration on the water-air interface in a soil sample
M(t) (mg) Mass of dissolved O_2 on the water-air interface in a soil sample at time t
ξ (cm) A dimension matching parameter
Θ Soil saturation
R_e(t) (μg s^{-1}) Microbial reduction rate of dissolved O_2 at time t from a soil sample
s (s^{-1}) Laplace transform variable
a (s^{-1}) Soil parameter characterising the memory function

β Soil parameter characterising the memory function
b Soil parameter characterising the memory function
$R_0(\theta)$ ($\mu g\ s^{-1}$) Steady microbial respiration from a soil sample when soil water content is θ
a_1 (s) Soil parameter characterising the memory function
θ_s Soil porosity
A_0 (cm^2) Parameter characterising the change in water-air interfacial area with saturation
b_1 Parameter characterising the change in water-air interfacial area with saturation
b_2 Parameter characterising the change in water-air interfacial area with saturation
q ($\mu g\ cm^{-2}\ s^{-1}$) O_2 dissolution rate over a unit area of the water-air interface
κ ($cm\ s^{-1}$) O_2 dissolution rate coefficient on over a unit area of the water-air interface
C_{eq} ($mg\ L^{-1}$) Saturated dissolved O_2 concentration calculated from Henry's law
E_a ($k\ J\ mol^{-1}$) Activation energy of soil substrates in the Arrhenius equation
λ (s^{-1}) The pro-exponential factor in the Arrhenius equation (Respiration rate from a unit weight of soil)
R ($J\ K^{-1}\ mol^{-1}$) The gas constant
T (K) Temperature
λ_0 (s^{-1}) The pro-exponential factor after being modified by soil water content (respiration rate from a unit weight of soil)
α_1 Soil parameter characterising pore-scale substrate accessibility
γ_1 Soil parameter characterising pore-scale substrate accessibility
ε Porosity of macropores
α_0 (s) Soil parameter characterising the impact of clay on memory function
S_c ($mg\ mg^{-1}$) Clay content
η_0 ($\mu g\ s^{-1}$) Potential respiration rate of each microbe
K_c ($mg\ mg^{-1}$) Affinity parameter for impact of clay on pore-scale substrate accessibility
γ_0 Soil parameter for impact of clay on substrate accessibility
ε_0 Soil parameter for impact of clay on porosity of macropores
n Average numbers of microbes at the micro-reactive sites
S ($mg\ L^{-1}$) Substrate abundance
K_S ($mg\ L^{-1}$) Affinity parameter for substrates

Appendix A. Supplementary data

Supplementary data to this article can be found online at https://doi.org/10.1016/j.soilbio.2023.109147.

References

Azizi-Rad, M., Guggenberger, G., Ma, Y., Sierra, C.A., 2022. Sensitivity of soil respiration rate with respect to temperature, moisture and oxygen under freezing and thawing. Soil Biology and Biochemistry 165, 108488.

Bacq-Labreuil, A., Crawford, J., Mooney, S.J., Neal, A.L., Akkari, E., McAuliffe, C., Zhang, X.X., Redmile-Gordon, M., Ritz, K., 2018. Effects of cropping systems upon the three-dimensional architecture of soil systems are modulated by texture. Geoderma 332, 73–83.

Bailey, V.L., Pries, C.H., Lajtha, K., 2019. What do we know about soil carbon destabilization? Environmental Research Letters 14, 083004.

Bailey, V.L., Smith, A.P., Tfaily, M., Fansler, S.J., Bond-Lamberty, B., 2017. Differences in soluble organic carbon chemistry in pore waters sampled from different pore size domains. Soil Biology and Biochemistry 107, 133–143.

Bauer, J., Herbst, M., Huisman, J.A., Weihermuller, L., Vereecken, H., 2008. Sensitivity of simulated soil heterotrophic respiration to temperature and moisture reduction functions. Geoderma 145, 17–27.

Beven, K., Germann, P., 2013. Macropores and water flow in soils revisited. Water Resources Research 49, 3071–3092.

Chakrawal, A., Herrmann, A.M., Koestel, J., Jarsjö, J., Nunan, N., Kätterer, T., Manzoni, S., 2020. Dynamic upscaling of decomposition kinetics for carbon cycling models. Geoscientific Model Development 13, 1399–1429.

Chen, W., Wagenet, R.J., 1997. Description of atrazine transport in soil with heterogeneous nonequilibrium sorption. Soil Science Society of America Journal 61, 360–371.

Coats, K.H., Smith, B.D., 1964. Dead-end pore volume and dispersion in porous media. Society of Petroleum Engineers Journal 4, 73–84.

Curiel Yuste, J., Baldocchi, D.D., Gershenson, A., Goldstein, A., Misson, L., Wong, S., 2007. Microbial soil respiration and its dependency on carbon inputs, soil temperature and moisture. Global Change Biology 13, 2018–2035.

Cvetkovic, V., 2012. A general memory function for modeling mass transfer in groundwater transport. Water Resources Research 48.

Davidson, E.A., 2020. Carbon loss from tropical soils increases on warming. Nature 584, 198–199.

Davidson, E.A., Janssens, I.A., 2006. Temperature sensitivity of soil carbon decomposition and feedbacks to climate change. Nature 440, 165–173.

Davidson, E.A., Samanta, S., Caramori, S.S., Savage, K., 2012. The Dual Arrhenius and Michaelis-Menten kinetics model for decomposition of soil organic matter at hourly to seasonal time scales. Global Change Biology 18, 371–384.

de Nijs, E.A., Hicks, L.C., Leizeaga, A., Tietema, A., Rousk, J., 2019. Soil microbial moisture dependences and responses to drying–rewetting: the legacy of 18 years drought. Global Change Biology 25, 1005–1015.

Ebrahimi, A., Or, D., 2016. Microbial community dynamics in soil aggregates shape biogeochemical gas fluxes from soil profiles - upscaling an aggregate biophysical model. Global Change Biology 22, 3141–3156.

Faisal Anwar, A.H.M., Bettahar, M., Matsubayashi, U., 2000. A method for determining air–water interfacial area in variably saturated porous media. Journal of Contaminant Hydrology 43, 129–146.

Falloon, P., Jones, C.D., Ades, M., Paul, K., 2011. Direct soil moisture controls of future global soil carbon changes: an important source of uncertainty. Global Biogeochemical Cycles 25, GB3010.

Fang, C., Moncrieff, J.B., 2001. The dependence of soil CO_2 efflux on temperature. Soil Biology and Biochemistry 33, 155–165.

Franklin, S.M., Kravchenko, A.N., Vargas, R., Vasilas, B., Fuhrmann, J.J., Jin, Y., 2021. The unexplored role of preferential flow in soil carbon dynamics. Soil Biology and Biochemistry 161, 108398.

Franzluebbers, A.J., 1999. Microbial activity in response to water-filled pore space of variably eroded southern Piedmont soils. Applied Soil Ecology 11, 91–101.

Guilhen, J., Al Bitar, A., Sauvage, S., Parrens, M., Martinez, J.M., Abril, G., Moreira-Turcq, P., Sánchez-Pérez, J.M., 2020. Denitrification and associated nitrous oxide and carbon dioxide emissions from the Amazonian wetlands. Biogeosciences 17, 4297–4311.

Haaf, D., Six, J., Doetterl, S., 2021. Global patterns of geo-ecological controls on the response of soil respiration to warming. Nature Climate Change 11, 623–627.

Haggerty, R., Gorelick, S.M., 1995. Multi-rate and multi-transfer for modelling diffusion and surface-reaction in media with pore-scale heterogeneity. Water Resources Research 31, 2383–2400.

Harris, E., Diaz-Pines, E., Stoll, E., Schloter, M., Schulz, S., Duffner, C., Li, K., Moore, K.L., Ingrisch, J., Reinthaler, D., Zechmeister-Boltenstern, S., Glatzel, S., Brüggemann, N., Bahn, M., 2021. Denitrifying pathways dominate nitrous oxide emissions from managed grassland during drought and rewetting. Science Advances 7, eabb7118.

Hawkes, C.V., Waring, B.G., Rocca, J.D., Kivlin, S.N., 2017. Historical climate controls soil respiration responses to current soil moisture. Proc. Natl. Acad. Sci. U.S.A. 114, 6322–6327.

Herbst, M., Tappe, W., Kummer, S., Vereecken, H., 2016. The impact of sieving on heterotrophic respiration response to water content in loamy and sandy topsoils. Geoderma 272, 73–82.

Hu, W.L., Huang, N., Zhang, X.X., 2014. Impact of saturation on mass transfer rate between mobile and immobile waters in solute transport within aggregated soils. Journal of Hydrology 519, 3557–3565.

Keiluweit, M., Wanzek, T., Kleber, M., Nico, P., Fendorf, S., 2017. Anaerobic microsites have an unaccounted role in soil carbon stabilization. Nature Communications 8, 1771.

Kravchenko, A.N., Guber, A.K., Razavi, B.S., Koestel, J., Blagodatskaya, E.V., Kuzyakov, Y., 2019a. Spatial patterns of extracellular enzymes: combining X-ray computed micro-tomography and 2D zymography. Soil Biology and Biochemistry 135, 411–419.

Kravchenko, A.N., Guber, A.K., Razavi, B.S., Koestel, J., Quigley, M.Y., Robertson, G.P., Kuzyakov, Y., 2019b. Microbial spatial footprint as a driver of soil carbon stabilization. Nature Communications 10, 3121.

Lee, E.S., Birkham, T.K., Wassenaar, L.I., Hendry, M.J., 2003. Microbial respiration and diffusive transport of O_2, $^{16}O_2$, and $^{18}O^{16}O$ in unsaturated soils and geologic sediments. Environmental Science and Technology 37, 2913–2919.

Li, J.-T., Zhang, Y., Chen, H., Sun, H., Tian, W., Li, J., Liu, X., Zhou, S., Fang, C., Li, B., Nie, M., 2023. Low soil moisture suppresses the thermal compensatory response of microbial respiration. Global Change Biology 29, 874–889.

Li, Z., Zhang, X., Liu, Y., 2017. Pore-scale simulation of gas diffusion in unsaturated soil aggregates: Accuracy of the dusty-gas model and the impact of saturation. Geoderma 303, 196–203.

Li, Z.Y., Zhang, X.X., Wang, D., Liu, Y., 2018. Direct methods to calculate the mass exchange between solutes inside and outside aggregates in macroscopic model for solute transport in aggregated soil. Geoderma 320, 126–135.

Liang, J., Chen, K., Siqintana, Huo, T., Zhang, Y., Jing, J., Feng, W., 2022. Towards improved modeling of SOC decomposition: soil water potential beyond the wilting point. Global Change Biology 28, 3665–3673.

Linn, D.M., Doran, J.W., 1984. Effect of water-filled pore space on carbon-dioxide and nitrous-oxide production in tilled and nontilled soils. Soil Science Society of America Journal 48, 1267–1272.

Liu, W.X., Zhang, Z., Wan, S.Q., 2009. Predominant role of water in regulating soil and microbial respiration and their responses to climate change in a semiarid grassland. Global Change Biology 15, 184–195.

Manzoni, S., Moyano, F., Katterer, T., Schimel, J., 2016. Modeling coupled enzymatic and solute transport controls on decomposition in drying soils. Soil Biology and Biochemistry 95, 275–287.

Moyano, F.E., Manzoni, S., Chenu, C., 2013. Responses of soil heterotrophic respiration to moisture availability: an exploration of processes and models. Soil Biology and Biochemistry 59, 72–85.

Reichstein, M., Rey, A., Freibauer, A., Tenhunen, J., Valentini, R., Banza, J., Casals, P., Cheng, Y., Grünzweig, J.M., Irvine, J., Joffre, R., Law, B.E., Loustau, D., Miglietta, F., Oechel, W., Ourcival, J.-M., Pereira, J.S., Peressotti, A., Ponti, F., Qi, Y., Rambal, S., Rayment, M., Romanya, J., Rossi, F., Tedeschi, V., Tirone, G., Xu, M., Yakir, D., 2003. Modeling temporal and large-scale spatial variability of soil respiration from soil water availability, temperature and vegetation productivity indices. Global Biogeochemical Cycles 17, 1104.

Schimel, J., 2023. Modeling ecosystem-scale carbon dynamics in soil: the microbial dimension. Soil Biology and Biochemistry 178, 108948.

Sierra, C.A., Malghani, S., Loescher, H.W., 2017. Interactions among temperature, moisture, and oxygen concentrations in controlling decomposition rates in a boreal forest soil. Biogeosciences 14, 703–710.

Sierra, C.A., Trumbore, S.E., Davidson, E.A., Vicca, S., Janssens, I., 2015. Sensitivity of decomposition rates of soil organic matter with respect to simultaneous changes in temperature and moisture. Journal of Advances in Modeling Earth Systems 7, 335–356.

Skopp, J., Jawson, M.D., Doran, J.W., 1990. Steady-state aerobic microbial activity as a function of soil water content. Soil Science Society of America Journal 54, 1619–1625.

Sun, W., Peppley, B.A., Karan, K., 2005. An improved two-dimensional agglomerate cathode model to study the influence of catalyst layer structural parameters. Electrochimica Acta 50, 3359–3374.

Tang, J., Riley, W.J., 2019. A theory of effective microbial substrate affinity parameters in variably saturated soils and an example Application to aerobic soil heterotrophic respiration. Journal of Geophysical Research: Biogeosciences 124, 918–940.

Tokida, T., Adachi, M., Cheng, W., Nakajima, Y., Fumoto, T., Matsushima, M., Nakamura, H., Okada, M., Sameshima, R., Hasegawa, T., 2011. Methane and soil CO_2 production from current-season photosynthates in a rice paddy exposed to elevated CO_2 concentration and soil temperature. Global Change Biology 17, 3327–3337.

Wilson, C.H., Gerber, S., 2021. Theoretical insights from upscaling Michaelis–Menten microbial dynamics in biogeochemical models: a dimensionless approach. Biogeosciences 18, 5669–5679.

Yan, Z.F., Bond-Lamberty, B., Todd-Brown, K.E., Bailey, V.L., Li, S.L., Liu, C.Q., Liu, C.X., 2018. A moisture function of soil heterotrophic respiration that incorporates microscale processes. Nature Communications 9, 2562.

Yan, Z.F., Liu, C.X., Todd-Brown, K.E., Liu, Y.Y., Bond-Lamberty, B., Bailey, V.L., 2016. Pore-scale investigation on the response of heterotrophic respiration to moisture conditions in heterogeneous soils. Biogeochemistry 131, 121–134.

Zhang, X., Whalley, P.A., Gregory, A.S., Whalley, W.R., Coleman, K., Neal, A.L., Mooney, S.J., Soga, K., Illangasekare, T.H., 2022. An overlooked mechanism underlying the attenuated temperature response of soil heterotrophic respiration. Journal of the Royal Society Interface 19, 20220276.

Zhang, X.X., Gao, Y., 2016. Impact of liquid water on oxygen reaction in cathode catalyst layer of proton exchange membrane fuel cell: a simple and physically sound model. Journal of Power Sources 318, 251–263.

Zhang, X.X., Gao, Y., Ostadi, H., Jiang, K.L., Chen, R., 2014. A proposed agglomerate model for oxygen reduction in the catalyst layer of proton exchange membrane fuel cells. Electrochimica Acta 150, 320–328.

Zheng, J., Bond-Lamberty, B., Bailey, V., 2022. Revisiting diffusion-based moisture functions: why do they fail? Soil Biology and Biochemistry 165, 108525.

Zhou, W.P., Hui, D.F., Shen, W.J., 2014. Effects of soil moisture on the temperature sensitivity of soil heterotrophic respiration: a laboratory incubation study. PLoS One 9, 10.

Zoia, A., Neel, M.C., Cortis, A., 2010. Continuous-time random-walk model of transport in variably saturated heterogeneous porous media. Physical Review E 81, 031104.